Electron paramagnetic resonance investigation of Dy^{3+} ions in $Bi_4Ge_3O_{12}$ single crystals

Electron paramagnetic resonance investigation of Dy^{3+} ions in $Bi_4Ge_3O_{12}$ single crystals

D Bravo†, A A Kaminskii‡ and F J López†

† Departamento de Física de Materiales, Facultad de Ciencias, C-IV, Universidad Autónoma de Madrid, E-28049 Madrid, Spain
‡ A V Shubnikov Institute of Crystallography, Russian Academy of Sciences, Moscow 117333, Russia

Abstract. An X-band electron paramagnetic resonance study at 5 K of Dy^{3+} ions in $Bi_4Ge_3O_{12}$ single crystals is reported. The spectra have been attributed to a unique centre of Dy^{3+} located at the Bi^{3+} site. The spin-Hamiltonian parameters have been determined for the even isotopes of Dy, as well as for the isotopes ^{161}Dy and ^{163}Dy. Moreover, a detailed g-factor analysis has been carried out by obtaining the ground doublet wavefunction. To this purpose, we have employed an interpolated set of crystal-field B_n^m parameters for Dy^{3+} which was estimated from the fitted B_n^m sets of Nd^{3+} and Er^{3+} in $Bi_4Ge_3O_{12}$. It is found that the interpolated set yields a satisfactory approach to the experimental g-factor values, which makes it feasible to predict the energy-level scheme for the ground manifold $^6H_{15/2}$ of Dy^{3+} in this host.

1. Introduction

Single crystals of $Bi_4Ge_3O_{12}$ (or BGO) have primarily been of interest as particle scintillation detectors since they present a highly efficient luminescence [1]. Also, BGO has attracted attention owing to its applications in non-linear optical devices [2, 3] and is known to be a good candidate for making low-loss He^+-implanted waveguides [4]. In addition, BGO is a potential solid state laser host when activated with trivalent rare-earth (RE) ions, in bulk [5–7] and waveguide structures [4]. One attractive aspect of rare-earth BGO laser systems is the possibility of enhanced pumping of the active ions through host absorption and energy transfer, where constituent Bi^{3+} ions act as effective luminescence sensitizers for some RE ions [8, 9].

As with any laser crystal, determination of the crystal-field (CF) energy levels of the active ion in BGO is the first stage of study to gain a better understanding of the physics of the stimulated-emission processes. To this purpose, Kaminskii *et al* [5–7] carried out extensive investigations on several RE ions in BGO by optical spectroscopy and obtained the energy level schemes of Nd^{3+} [5], Er^{3+}, Yb^{3+} [6] and Pr^{3+} [7] in this host. The second stage of study implies determining the point symmetry group of the site occupied by the RE ion and the symmetry properties of the energy-level wavefunctions. At this point one must consider the crystal structure of $Bi_4Ge_3O_{12}$, which belongs to the cubic space group $I\bar{4}3d$ [6, 10]. In this lattice, each Ge^{4+} ion has S_4 site symmetry and is coordinated by four oxygen ions arranged in a tetrahedron slightly distorted along a $\langle 100 \rangle$ crystal direction, whereas each Bi^{3+} ion is coordinated by six oxygen ions in a site with C_3 symmetry; in this case the distortion and the corresponding threefold axis take place along a $\langle 111 \rangle$ direction of the cubic cell.

For the BGO laser host Morrison and Leavitt [11] have analysed the energy-level structure for Er^{3+} and Nd^{3+} by fitting the experimental data with the appropriate sets of crystal-field B_n^m parameters and assuming C_3 point symmetry. In that work [11] sets of 'smoothed' B_n^m parameters for the entire lanthanide series are also provided, which have been estimated from the fitted B_n^m sets for Nd^{3+} and Er^{3+} in BGO. We have recently tested [12] the 'smoothed' set for Yb^{3+} given in [11] and found that it gives a rough but satisfactory approach to the experimental crystal-field levels obtained in [6] and g-factor values measured in [12] by means of the electron paramagnetic resonance (EPR) technique.

The EPR technique has been particularly useful to determine the location, and then the site symmetry, of the RE ions Gd^{3+} [13], Er^{3+} [14], Nd^{3+} [15] and Yb^{3+} [12] in BGO, as well as to investigate the physical properties of their ground state by correlating the EPR and optical results [12, 14, 15]. All investigated RE ions have been found by EPR at the Bi^{3+} site (point symmetry C_3). This agrees with the assumption in the work of Morrison and Leavitt [11], since the energy-level schemes of Er^{3+} and Nd^{3+} are satisfactorily explained by means of a CF Hamiltonian for C_3 symmetry.

From the quoted results for several RE ions in BGO, one would expect that the laser ion Dy^{3+} [16] also occupies the Bi^{3+} site. This is confirmed in the present work by means of the EPR technique. Moreover, the spin-Hamiltonian parameters for Dy^{3+} in BGO are determined and the experimental g-factor values are analysed by means of crystal-field theory. It is found here that the 'smoothed' B_n^m set given in [11] for Dy^{3+} gives calculated g-factor values very close to the experimental ones, with better agreement than for Yb^{3+} [12] as mentioned above. In view of the consistent results and taking into account that the energy-level scheme for the ground manifold $^6H_{15/2}$ of Dy^{3+} in BGO, as well as the symmetry properties of the corresponding wavefunctions, are not available in the literature, we have also employed the 'smoothed' set to predict them.

2. Experiment

Single crystals of BGO have been grown from the melt by the Czochralski technique. Details of the growth procedure have been given elsewhere [6]. A $\approx 1\%$ molar concentration of Dy impurities was added to the starting growth materials, so that a concentration of about 0.8% in the crystals is expected from the effective distribution coefficient of Dy in BGO [6]. From the boule obtained, a sample of 2 mm $\times$ 2 mm $\times$ 6 mm was cut and oriented by taking a number of Laue x-ray diffraction patterns.

A Bruker ESP 300 E X-band spectrometer with field modulation of 100 kHz was used to record the EPR spectra. The temperature of the sample was controlled by means of a continuous-flow liquid-helium cryostat (Oxford Instruments ESR 900). Accurate values of the resonance magnetic fields and microwave frequencies were measured with a NMR gaussmeter (Bruker ER 035 M) and a frequency meter (Hewlett–Packard 5342A), respectively. The sample was mounted on a goniometer for measurements of the angular variation of the EPR spectra.

3. Results

The EPR spectrum of Dy-doped BGO crystals has been measured at 5 K and consists of a maximum of four groups of lines. Each group is formed by an intense central line surrounded by various weaker components, as observed in figure 1 for the EPR spectrum obtained with the magnetic field B parallel to a $\langle 100 \rangle$ crystal direction. For this orientation

of B the four groups have collapsed into a single one. It is observed that the components and the intense central line undergo similar splittings as the orientation of B with respect to the crystal axes of BGO is changed. Therefore, we attribute the weaker components to 'allowed' hyperfine transitions (with $\Delta m = 0$, where m is the nuclear magnetic quantum number) which arise from the odd isotopes of dysprosium, ^{161}Dy and ^{163}Dy, both having nuclear spin $I = 5/2$. Thus, the intense central line comes from the even isotopes with $I = 0$. This assignment will be confirmed from the experimental hyperfine parameters for both isotopes, which are determined below.
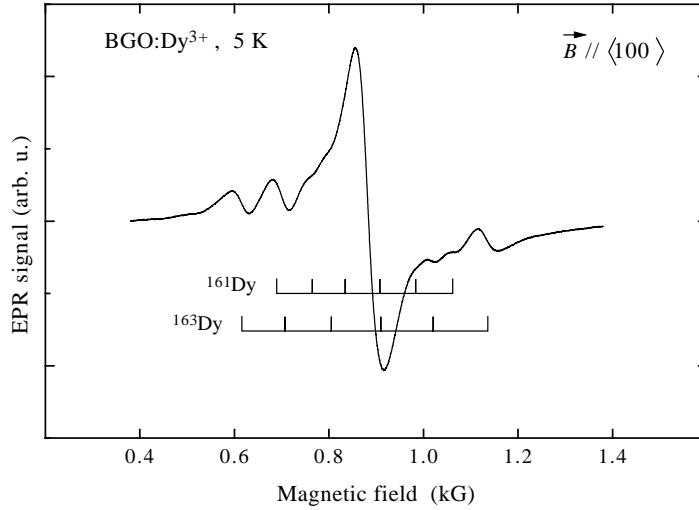

Figure 1. EPR spectrum of Dy-doped $Bi_4Ge_3O_{12}$ single crystals measured at 5 K with the magnetic field B parallel to a $\langle 100 \rangle$ crystal direction. Stick diagrams in the lower part of the figure depict the resonance fields for the 'allowed' hyperfine transitions of ^{161}Dy and ^{163}Dy as calculated with the parameters in table 1. All the lines are fourfold degenerate for this orientation of B.

The angular dependence of the EPR spectrum has been studied for B lying in a {110} crystal plane and has been plotted in figure 2. While B is rotated in this plane, each line of the fourfold degenerate group (shown in figure 1 and in figure 2 at $\Psi = 0°$) splits and moves as two single lines and one doubly degenerate line. This is evidenced by tilting the sample out of that plane. The doubly degenerate lines are identified in figure 2 as those taking extreme values of their resonance fields at the [001] and [110] orientations. For the sake of clarity only the low-field region of the angular dependence is shown in figure 2. Nevertheless, EPR lines strongly dependent on orientation were measured up to 13 kG for orientations of B close to the [111] crystal direction (at $\Psi = 54.74°$ in figure 2) where it is expected they reach the absolute maximum value of the resonance field.

The EPR spectrum and its angular dependence are characteristic of a defect with effective spin $S' = 1/2$ having axial symmetry along the $\langle 111 \rangle$ crystal directions. The four intense central lines and their respective accompanying hyperfine groups observed for arbitrary orientations of B are associated with the four magnetically inequivalent orientations of a single dysprosium centre with axial symmetry along the $\langle 111 \rangle$ directions of the cubic lattice of BGO. Therefore, the EPR spectra has been analysed by means of the following spin Hamiltonian ($S' = 1/2$ and $I = 5/2$):

$$\hat{\mathcal{H}} = g_{\parallel}\mu_B B_Z \hat{S}'_Z + g_{\perp}\mu_B(B_X \hat{S}'_X + B_Y \hat{S}'_Y) + A_{\parallel}\hat{S}'_Z \hat{I}_Z + A_{\perp}(\hat{S}'_X \hat{I}_X + \hat{S}'_Y \hat{I}_Y). \tag{1}$$
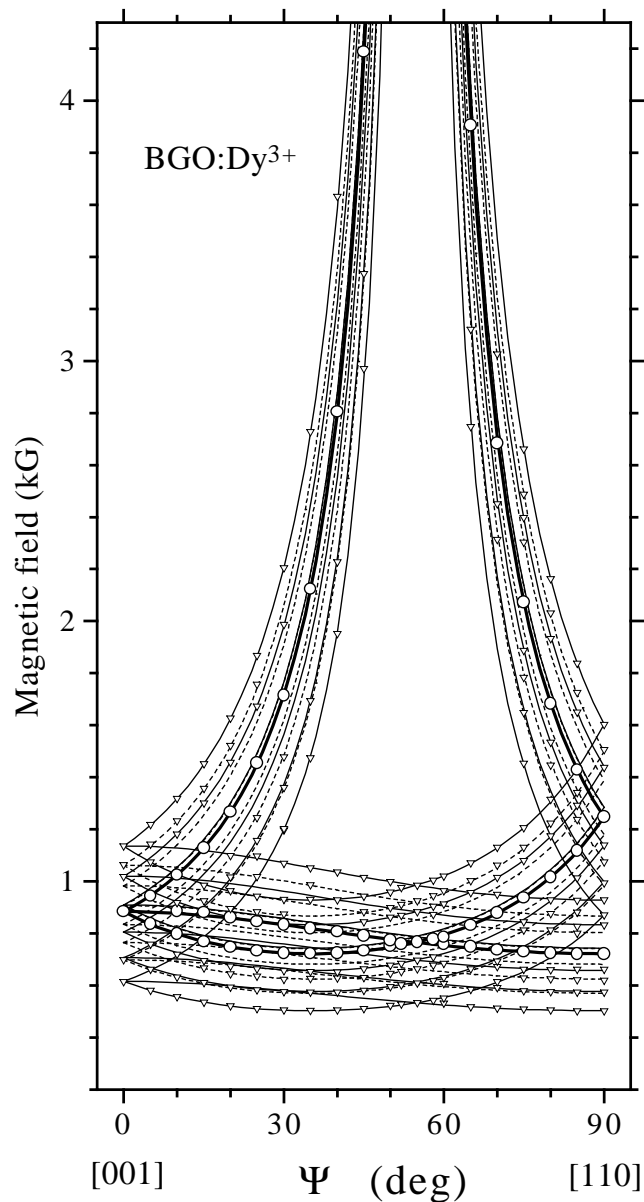
Figure 2. Angular variation of the EPR spectrum of Dy-doped $Bi_4Ge_3O_{12}$ measured at 5 K, with B lying in a {110} crystal plane and forming an angle Ψ with the [001] direction. Big circles and triangles show the experimental resonance positions of the even and odd isotope EPR lines, respectively. The high-field region of the angular variation (up to 14 kG) has not been included to better observe the hyperfine structure (see text). The calculated angular variation for the even-isotope lines is plotted with thick continuous lines. Thin continuous and dashed lines are used for the 'allowed' $\Delta m = 0$ hyperfine transitions of ^{163}Dy and ^{161}Dy, respectively.

In this expression, X, Y and Z are the defect principal axes, Z being chosen parallel to a $\langle 111 \rangle$ direction. The parameters in the Zeeman and hyperfine structure terms have the usual meaning. The full spin Hamiltonian is used to study the ^{161}Dy and ^{163}Dy resonances,

whereas only the Zeeman part is necessary for the even-isotope lines. No quadrupole term has been considered in equation (1) for the odd isotopes since it mainly affects the resonance position of so-called 'forbidden' transitions (e.g. with $\Delta m = \pm 1$ or ± 2) [17], which are not observed in the spectra.

The analysis of the EPR spectra has been carried out by numerical diagonalization of the corresponding energy matrix for each isotope. Each matrix is constructed for a given set of parameters $g_\parallel$, $g_\perp$, $A_\parallel$ and $A_\perp$ and for different orientations of the defect axis with respect to the magnetic field. In this way, accurate values for the resonance fields are calculated. The values for $g_\parallel$ and $g_\perp$, given in table 1, are readily obtained from the positions of the even-isotope lines. Note that the accuracy for $g_\parallel$ is low, which is due to the experimental fact that the high-field lines (for B close to the [111] direction) become very broad. The $g_\parallel$ and $g_\perp$ values are kept fixed in the analysis of the odd-isotope hyperfine components, and the parameters $A_\parallel$ and $A_\perp$ for each odd isotope are obtained from a least-squares method. The best fits for the hyperfine components are reached with the parameter sets listed in table 1.

Table 1. Spin-Hamiltonian parameters measured for Dy^{3+} in Bi$_4$Ge$_3$O$_{12}$. Signs for $g_\parallel$ and $A_\parallel$ are determined by theory (see text). Hyperfine parameters are given in units of 10^{-4} cm^{-1}.

$g_\parallel$	$|g_\perp|$	Isotope	$A_\parallel$	$|A_\perp|$
		^{161}Dy	-11 ± 3	259 ± 3
$+0.4 \pm 0.1$	9.349 ± 0.008			
		^{163}Dy	$+16 \pm 4$	370 ± 2

It is worth noting that the sign for $g_\parallel$ has been taken positive as follows from the analysis of the ground state wavefunction of Dy^{3+} carried out in the next section. This implies that the sign for $A_\parallel$ must be taken negative for ^{161}Dy and positive for ^{163}Dy as a consequence of the relation $A_\parallel / g_\parallel \cong A_\perp / g_\perp \cong A_J / g_J$ [17], where A_J and g_J are the corresponding magnetic hyperfine constant and the Landé g-factor for the ground level of the free ion ^{161}Dy^{3+} and ^{163}Dy^{3+}, respectively. On the other hand, only the absolute value for $g_\perp$ and, consequently for $A_\perp$, can be determined [17].

Using the parameter sets given in table 1, the resonance fields corresponding to the four $\langle 111 \rangle$ orientations of the dysprosium defect in BGO have been calculated. The theoretical angular variation has been plotted in figure 2 with thick continuous lines for the even-isotope lines, whereas thin continuous and dashed lines are used for the sextets of 'allowed' hyperfine transitions of ^{163}Dy and ^{161}Dy, respectively. As observed in figure 2, the agreement with experiment is very satisfactory.

4. Discussion and analysis

In order to confirm that we are dealing with Dy impurities in BGO, the experimental ratios between the hyperfine constants of both isotopes are now compared to the ratio between the corresponding nuclear magnetic moments μ. From table 1 one obtains $^{163}A_\parallel / {}^{161}A_\parallel = -1.5 \pm 0.8$ and $^{163}A_\perp / {}^{161}A_\perp = -1.43 \pm 0.02$, whereas $^{163}\mu / {}^{161}\mu = -1.407$, in good agreement. Furthermore, the facts that the effective spin is $S' = 1/2$ and the mean g-value is $\bar{g} = (g_\parallel + 2g_\perp)/3 = 6.37$ indicate that dysprosium is in the trivalent state [17].

On the other hand, the observed axiality of the dysprosium defect along the $\langle 111 \rangle$ crystal directions can be explained assuming that Dy^{3+} substitutes for Bi^{3+}, because only the Bi^{3+}

sites have such symmetry, as mentioned in section 1. Thus, this result confirms the location of Dy^{3+} in BGO, in agreement with the proposal of Kaminskii *et al* [6] and Morrison and Leavitt [11].

4.1. Analysis of g-factor values

The electronic configuration of Dy^{3+} is $4f^9$ with a free-ion ground level $^6H_{15/2}$ in the Russell-Saunders notation. The ground level splits into eight Kramers' doublets for crystal fields whose symmetry is lower than cubic [18] (trigonal C_3 in the present case). In general, the splitting is large enough so that only the lowest-lying doublet will be appreciably populated at low temperatures. Thus, the observed EPR signals arise only from the ground doublet, which has been described above by means of an effective spin $S' = 1/2$ [19].

Theoretical principal g-values for a Kramers' doublet can be calculated with the following expressions [17,19]:

$$g_\parallel = 2g_J \langle +|\hat{J}_Z|+\rangle$$
$$g_\perp = g_J \langle +|\hat{J}_+|-\rangle \tag{2}$$

where g_J is the Landé g-factor for the ground level $^6H_{15/2}$ of the free Dy^{3+} ion. The wavefunctions $|+\rangle$ and $|-\rangle$ describe the two states of the Kramers' doublet which are linear combinations of $|M_J\rangle$ states as a consequence of the crystal field. In our case, the threefold nature of the crystal field will result in admixtures of states whose M_J values differ by ± 3. In this way, the ground-doublet wavefunction will be associated with the crystal quantum numbers either $q = \pm 1/2$ or $q = \pm 3/2$ [17, 20]. From the analysis carried out below one ascertains that $q = \pm 1/2$, so that the doublet will be [14, 17]:

$$|+\rangle = a|+13/2\rangle + b|+7/2\rangle + c|+1/2\rangle + d|-5/2\rangle + e|-11/2\rangle$$
$$|-\rangle = -a^*|-13/2\rangle + b^*|-7/2\rangle - c^*|-1/2\rangle + d^*|+5/2\rangle - e^*|+11/2\rangle \tag{3}$$

where the coefficients a, b, c, d and e are complex as a result of the C_3 symmetry of the site occupied by Dy^{3+}, and the asterisk (*) means the complex conjugate.

In order to obtain theoretical g-factor values with equations (2) and (3), knowledge of the five coefficients for the ground-doublet wavefunction is necessary. With this aim, the 16×16 crystal-field (CF) energy matrix for the ground $J = 15/2$ manifold of Dy^{3+} is constructed using the operator equivalent technique [17, 19], as detailed in previous publications [14, 15]. The employed CF Hamiltonian is as follows:

$$\hat{\mathcal{H}}_{CF} = \sum_{n,m} B_n^m \langle J|x_n|J\rangle \hat{O}_n^m \tag{4}$$

where $\hat{O}_n^m$ are the Stevens operator equivalents, and $\langle J|x_n|J\rangle = \alpha$, β or γ for $n = 2$, 4 or 6, respectively, are the operator equivalent factors for the ground $J = 15/2$ manifold of Dy^{3+} [17].

It must be noted that the approximation here used of considering only the ground manifold of Dy^{3+} should be adequate to calculate the g-factor values, as follows from the work of Elliott and Stevens [19]. These authors show that admixtures from other higher-lying J manifolds may be neglected when the ratio $|g_\parallel A_\perp/g_\perp A_\parallel|$ takes a value near 1. This is fulfilled for Dy^{3+} in BGO, as the ratio calculated from the results in table 1 is 1.01 for ^{161}Dy and 0.99 for ^{163}Dy.

The CF energy matrix associated with the Hamiltonian of equation (4) has been constructed in the $|J, M_J\rangle$ free-ion basis, with $J = 15/2$, by using the 'smoothed' set of B_n^m parameters for Dy^{3+} in BGO given by Morrison and Leavitt [11]. As explained in

section 1, this set was estimated from those fitted for Nd^{3+} and Er^{3+}. The employed B_n^m parameters appropriate to the operator equivalent technique are shown in table 2. They have been translated (see [14] and references therein) from those given in [11], where the tensor operator technique [20] was used. Moreover, we have employed the following operator equivalent factors: $\alpha = -0.6217 \times 10^{-2}$, $\beta = -0.5865 \times 10^{-4}$ and $\gamma = 0.9773 \times 10^{-6}$ [21] which take into account the deviation from Russell–Saunders (LS) coupling for Dy^{3+}.

Table 2. 'Smoothed' crystal-field parameters B_n^m (cm⁻¹) for Dy^{3+} in $Bi_4Ge_3O_{12}$ translated from [11] to Stevens operator equivalent normalization (see text); $\Re$ and $\Im$ stand for real and imaginary parts, respectively. The ground-doublet coefficients a, b, c, d and e of equation (3) are listed as calculated with the 'smoothed' B_n^m. The calculated g-factor values are given together with the predicted crystal-field levels of the ground $^6H_{15/2}$ manifold and with the corresponding crystal quantum number q.

B_2^0	B_4^0	$\Re B_4^3$	B_6^0	$\Re B_6^3$	$\Im B_6^3$	$\Re B_6^6$	$\Im B_6^6$		
−385.5	−93.6	−4434	28.5	110.2	14.1	341.0	138.7		

	a	b	c	d	e				
$\Re$	−0.2135	0.5389	−0.5211	−0.5431	−0.3081				
$\Im$	−0.0064	0.0355	−0.0009	0.0359	0.0018				

	Energy levels (cm⁻¹)								$g_\parallel$	$\lvert g_\perp \rvert$
	0	32	78	202	328	403	469	671	+0.50	9.56
q	1/2	3/2	1/2	1/2	3/2	1/2	1/2	3/2		

Numerical diagonalization of the resulting complex matrix provides the energy level values for the $J = 15/2$ ground manifold (table 2) as well as the corresponding wavefunctions, which are included in the table in terms of crystal quantum numbers. The values for $g_\parallel$ and $g_\perp$ given in table 2 are calculated using the ground-doublet wavefunction (also given in the table) and the Landé g-factor $g_J = 1.323$ which results after considering deviations from LS coupling [22]. It is to be remarked that the calculated value for $g_\parallel$ turns out positive (e.g. see [14]). This determines the signs for $g_\parallel$ and $A_\parallel$ given in table 1, as mentioned above.

As observed, the 'smoothed' B_n^m parameters yield a good approach to the experimental g-factor values (table 1), the differences found being about 2% taking into account experimental errors. However, similar calculations carried out for Yb^{3+} in BGO [12] produced differences between experimental and calculated g-values of ≈20%. This is likely related to the remark in [11] that the 'smoothed' B_n^m do not give an accurate representation of the crystal-field splittings near the ends of the rare-earth series (Ce, Pr, Tm, Yb), but are quite accurate otherwise.

On the other hand, the analysis of the experimental g-factor values of Er^{3+} and Nd^{3+} carried out by Bravo *et al* [14, 15] has shown that the fitted sets of B_n^m parameters for these ions should be corrected, particularly some sixth-rank B_n^m. Therefore, one expects that the 'smoothed' sets for the remaining lanthanide ions should be corrected too, since they are obtained from the fitted sets for Er^{3+} and Nd^{3+}. So, the satisfactory results found here using the 'smoothed' set for Dy^{3+} would indicate that the faults in the B_n^m for Er^{3+} and Nd^{3+} compensate for Dy^{3+} via the smoothing method. In any case, since the faulty sixth-rank B_n^m for Er^{3+} and Nd^{3+} hardly affected their CF energy-level values [14, 15], the 'smoothed' set for Dy^{3+} should give a good approach not only to the ground-doublet wavefunction as found here, but also to the energy-level scheme and symmetry properties of the corresponding wavefunctions of Dy^{3+} in BGO. These data are predicted in table 2 for its $^6H_{15/2}$ ground manifold.

Acknowledgment

References

[1] Grabmaier B G 1984 *IEEE Trans. Nucl. Sci.* **NS-31** 372–6
[2] Kurz S K and Perry T T 1968 *J. Appl. Phys.* **39** 3798–813
[3] Montemezzani G, Pfändler St and Günter P 1992 *J. Opt. Soc. Am.* B **9** 1110–17
[4] Huang X, Jaque D, Vereda F, Fonrobert B, Chandler P J and Townsend P D 1996 *J. Mod. Opt.* **43** 1731–43
[5] Kaminskii A A, Schultze D, Hermoneit B, Sarkisov S E, Li L, Bohm J, Reiche P, Ehlert R, Mayer A A, Lomonov V A and Balashov V A 1976 *Phys. Status Solidi* a **33** 737–53
[6] Kaminskii A A, Sarkisov S E, Butaeva T I, Denisenko G A, Hermoneit B, Bohm J, Grosskreutz W and Schultze D 1979 *Phys. Status Solidi* a **56** 725–36
[7] Kaminskii A A, Sarkisov S E, Denisenko G A, Ryabchenkov V V, Lomonov V A, Perlin Yu E, Blazha M G, Schultze D, Hermoneit B and Reiche P 1984 *Phys. Status Solidi* a **85** 553–67
[8] Weber M J and Monchamp R R 1973 *J. Appl. Phys.* **44** 5495–9
[9] Neikirk P and Powell R C 1979 *J. Lumin.* **20** 261–70
[10] Segal D J, Santoro R P and Newnham R E 1966 *Z. Kristallogr.* **123** 73–6
[11] Morrison C A and Leavitt R P 1981 *J. Chem. Phys.* **74** 25–8
[12] Bravo D and López F J 1998 *Phys. Rev.* B at press
[13] Blanzat B, Raynal F, Parrot R, Barthou C and Canny B 1976 *Phys. Status Solidi* b **76** K5–K8
[14] Bravo D and López F J 1993 *J. Chem. Phys.* **99** 4952–9 and references therein
[15] Bravo D, Martín A, Kaminskii A A and López F J 1995 *Radiat. Eff. Defects Solids* **135** 191–4
[16] Kaminskii A A 1981 *Laser Crystals* (Berlin: Springer)
[17] Abragam A and Bleaney B 1970 *Electron Paramagnetic Resonance of Transition Ions* (Oxford: Clarendon)
[18] Lea K R, Leask M J M and Wolf W P 1962 *J. Phys. Chem. Solids* **23** 1381–405
[19] Elliott R J and Stevens K W H 1953 *Proc. R. Soc.* A **218** 553–66
[20] Wybourne B G 1965 *Spectroscopic Properties of Rare Earths* (New York: Wiley)
[21] Scott P D 1970 *PhD Thesis* Yale University
[22] Fry J L, Caspers H H, Rast H E and Miller S A 1968 *J. Chem. Phys.* **48** 2342—8